Macroscopic Quantum Synchronization Effects

Tobias Nadolny and Christoph Bruder
Department of Physics, University of Basel, Klingelbergstrasse 82, 4056 Basel, Switzerland

(Received 28 July 2023; accepted 16 October 2023; published 7 November 2023)

We theoretically describe macroscopic quantum synchronization effects occurring in a network of all-to-all coupled quantum limit-cycle oscillators. The coupling causes a transition to synchronization as indicated by the presence of global phase coherence. We demonstrate that the microscopic quantum properties of the oscillators qualitatively shape the synchronization behavior in a macroscopically large network. Specifically, they result in a blockade of collective synchronization that is not expected for classical oscillators. Additionally, the macroscopic ensemble shows emergent behavior not present at the level of two coupled quantum oscillators.

DOI: 10.1103/PhysRevLett.131.190402

In the presence of a sufficiently strong coupling, limit-cycle oscillators adjust their frequencies and exhibit coherence even in the presence of noise and disorder in their natural frequencies. This phenomenon is called synchronization; it appears, e.g., in physical, biological, engineered, and social systems [1–3] and has been extensively studied in classical nonlinear dynamics [4–8].

Recently, understanding synchronization of quantum oscillators has attracted a great deal of interest [9–64]. Quantum limit-cycle oscillators [10,11] can be implemented using harmonic oscillators [12–14] or few-level systems [15,16] supplemented by gain and loss. Experimental realizations span systems of cold atoms [17], nuclear spins [18], trapped ions [19], and a simulation on a quantum computer [20]. Large networks of quantum oscillators have been discussed, particularly two-level systems [21,22] and harmonic oscillators [12,13,23–30]. In most cases, their synchronization is similar to that of classical noisy oscillators. Some quantum features in such systems are discussed in Refs. [22–26], e.g., the presence of entanglement and quantum discord. Quantum effects beyond the influence of quantum noise that lead to a synchronization behavior qualitatively different from classical expectations have been studied mostly on the level of one, two, or three coupled oscillators [31–35].

So far, it has remained an open issue whether quantum effects in synchronization survive when increasing the number of oscillators. Will the quantum nature of the oscillators be reflected in the macroscopic dynamics? Or does the detailed microscopic description of each oscillator become irrelevant resulting in large-scale dynamics described by generic classical synchronization models? A third possibility is the emergence of behavior not visible at the level of few coupled oscillators.

In this Letter, we show how in a macroscopic ensemble of interacting quantum oscillators, the synchronization behavior is qualitatively shaped by their quantum nature. Both their wavelike character leading to interference and the discreteness of their energy levels result in quantum synchronization effects that remain visible in a large network. We explain these effects based on a comprehensive understanding of the behavior of each oscillator. In contrast, we identify aspects of the dynamics that are understood as typical synchronization transitions independently of the microscopic quantum properties. Finally, we discuss phase frustration in the network: if the coupling causes each oscillator to favor antialignment of its phase with respect to the other oscillators, collective synchronization is suppressed. This results in emergent blockades of synchronization only present in the many-body system.

Model.—To address the issue of quantum synchronization effects in large networks of oscillators, we consider the minimal model schematically shown in Fig. 1. It comprises two groups of oscillators and thus resembles models of two ensembles of classical phase oscillators [7,8]. Here, however, each group consists of quantum oscillators with three states $|0\rangle$, $|1\rangle$, and $|2\rangle$ each. In the frame rotating with the common frequency ω_z (see Fig. 1), the time evolution is governed by the quantum master equation $\dot{\rho} = -i[H_0 + H_{\mathrm{int}}, \rho] + \mathcal{L}\rho$, with

$$
\begin{aligned}
H_0 &= \sum_i \frac{\delta}{2}(S^z_{A,i} - S^z_{B,i}) + K\left(|2\rangle\langle 2|_{A,i} + |2\rangle\langle 2|_{B,i}\right) \\
H_{\mathrm{int}} &= \frac{V}{N}\sum_\sigma \sum_{i<j} S^+_{\sigma,i} S^-_{\sigma,j} + \frac{V_{AB}}{N}\sum_{i,j} S^+_{A,i} S^-_{B,j} + \mathrm{H.c.} \\
\mathcal{L} &= \sum_{\sigma,i}\left(\gamma_+ \mathcal{D}\left[|1\rangle\langle 0|_{\sigma,i}\right] + \gamma_- \mathcal{D}\left[|1\rangle\langle 2|_{\sigma,i}\right]\right). \qquad (1)
\end{aligned}
$$

In the sums, i and j take values from 1 to N and $\sigma \in \{A, B\}$ is the group label. The spin-1 operators are defined as $S^z = |2\rangle\langle 2| - |0\rangle\langle 0|$, $S^+ = \sqrt{2}(|2\rangle\langle 1| + |1\rangle\langle 0|)$, and

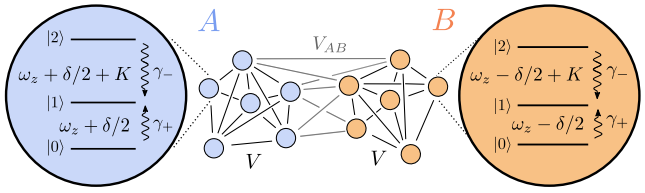

FIG. 1. Two groups A and B of N quantum oscillators each are all-to-all coupled through reactive interactions. Each oscillator consists of three levels and is incoherently driven to state $|1\rangle$. The asymmetry of the level structure is parametrized by K. The oscillators in group A are detuned from the ones in group B by δ.

$S^- = (S^+)^\dagger$. The Lindblad dissipator is $\mathcal{D}[o]\rho = o\rho o^\dagger - (o^\dagger o\rho + \rho o^\dagger o)/2$.

The bare Hamiltonian H_0 describes the coherent dynamics in the absence of any coupling. The two groups labeled A and B differ by the detuning δ between them. The parameter K sets the asymmetry in energy differences between levels $|2\rangle$ and $|1\rangle$, and the levels $|1\rangle$ and $|0\rangle$. The interaction among the oscillators is described by H_{int}. All oscillators are reactively coupled to all others. The coupling strength within each group is V, while the coupling strength between oscillators of different groups is V_{AB}. Finally, each three-level oscillator is incoherently driven to the level $|1\rangle$, with strength γ_+ (γ_-) from level $|0\rangle$ ($|2\rangle$). Because of these gain and loss processes, each three-level oscillator forms a limit cycle [15], whose population (measured by S^z) is stabilized, while the phase of the amplitude (measured by S^+) is free.

Because of the exponential growth of the Hilbert space size, solving the master equation becomes intractable for large N. We employ a mean-field treatment, which for the case of an all-to-all coupling discussed here gives an exact solution for the macroscopic dynamics in the limit $N \to \infty$ [65]. This approach corresponds to neglecting all correlations between operators, or, equivalently, using the product ansatz, $\rho = \bigotimes_{\sigma,i} \rho_{\sigma,i}$ [66]. Since all oscillators within each group are identical, their time evolution can be described in terms of two three-level oscillators with density matrices ρ_A and ρ_B coupled to the mean amplitudes $\langle S^+\rangle_\sigma = \mathrm{Tr}[\rho_\sigma S^+] = 1/N \sum_i \langle S^+_{\sigma,i}\rangle$ of each group. Consequently, the dynamics of the two groups is described by the two coupled nonlinear master equations

$$\begin{aligned}\dot\rho_A &= -i[H_A + V_{AB}(S^+\langle S^-\rangle_B + \text{H.c.}), \rho_A] + \tilde{\mathcal{L}}\rho_A,\\ \dot\rho_B &= -i[H_B + V_{AB}(S^+\langle S^-\rangle_A + \text{H.c.}), \rho_B] + \tilde{\mathcal{L}}\rho_B,\end{aligned} \tag{2}$$

where $H_\sigma = \pm(\delta/2)S^z + K|2\rangle\langle 2| + V(S^+\langle S^-\rangle_\sigma + \text{H.c.})$ and $\tilde{\mathcal{L}} = \gamma_+\mathcal{D}[|1\rangle\langle 0|] + \gamma_-\mathcal{D}[|1\rangle\langle 2|]$. The sign in front of $\delta/2$ is plus (minus) for group A (B). To obtain our results, we numerically time-integrate the nonlinear master equations (2). Additionally, we perform a stability analysis of the unsynchronized state $\rho_\sigma = |1\rangle\langle 1|$, which is a solution of $\dot\rho_\sigma = 0$.

Synchronization of a single group.—We begin to analyze the behavior of a single group by setting the intergroup coupling V_{AB} to zero. For simplicity, the group subscript $\sigma \in \{A, B\}$ is omitted in this section. To investigate the state of the group, we utilize the mean amplitude $\langle S^+\rangle = 1/N \sum_i \langle S_i^+\rangle$. The phase ϕ_i of each oscillator is defined through $\langle S_i^+\rangle = \exp(i\phi_i)|\langle S_i^+\rangle|$. In the absence of any coupling, all oscillators exhibit random phases due to the intrinsic quantum noise. Therefore, we expect the mean amplitude to vanish in the limit of infinitely many oscillators $N \to \infty$. This conclusion follows from the mean-field analysis by noting that for small coupling strength, the group of oscillators converges to the steady state $\rho = |1\rangle\langle 1|$ exhibiting no phase preference since $\langle S^+\rangle = 0$. The coupling among the oscillators, however, tends to align their phases. As in the Kuramoto model describing classical phase oscillators [4,67], there is a critical coupling strength V_c beyond which the group synchronizes. The critical coupling usually depends on both the noise and the frequency disorder inherent in the system. For a single group of identical oscillator, there is only intrinsic noise due to quantum fluctuations that increases with the rates γ_- and γ_+ at which each oscillator couples to the environment.

Figure 2(a) displays the time evolution of the mean amplitude in both the unsynchronized and synchronized regimes. Below the critical coupling strength, the zero-amplitude state is stable. For $V > V_c$, in the synchronized regime, the alignment of phases leads to a finite amplitude in the long-time limit with persistent oscillations of $\mathrm{Re}[\langle S^+\rangle]$. The frequency of this oscillation will be further addressed when discussing the behavior of two coupled groups. Other quantities not shown in Fig. 2(a) also change when entering the synchronized phase: the states $|0\rangle$ and $|2\rangle$ become populated, and the coherence $\langle |0\rangle\langle 2|\rangle$ exhibits oscillations at twice the frequency compared to those of $\langle S^+\rangle$.

To analyze the presence of synchronization among the oscillators, we use the time average of the (in general time-dependent) absolute value of the amplitude $|\langle S^+\rangle|_t$ in the steady state. Figure 2(b) depicts this order parameter as a function of the coupling strength, showing a sharp transition between the unsynchronized and synchronized states. This resembles transitions to continuous time crystals [68,69] or to superradiance [70] that also result from the competition of coherent and incoherent dynamics in open quantum systems.

So far, we set $\gamma_+/\gamma_- = 1/2$ and observed a typical synchronization transition. We now present the order parameter as a function of both the coupling strength and the ratio γ_+/γ_- in Fig. 2(c). Most notably, for equal gain and loss rates, the critical coupling diverges, i.e., the transition to synchronization disappears. This is a macroscopic manifestation of the interference blockade. Synchronization of a single three-level quantum limit-cycle oscillator subject to an external drive is suppressed when

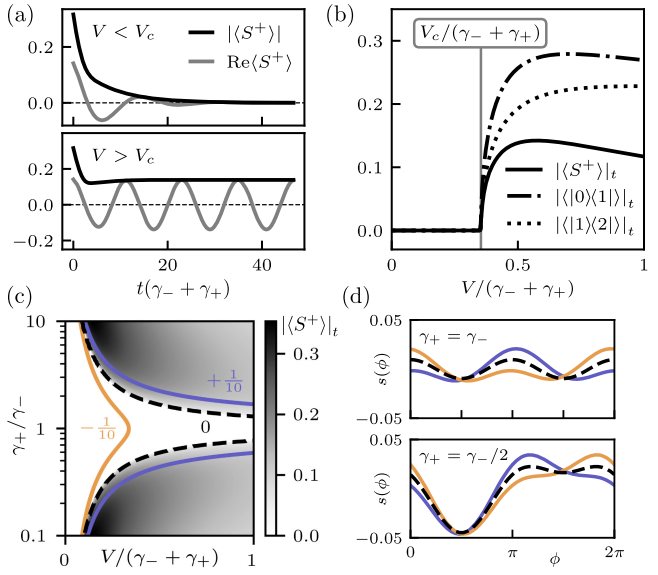

FIG. 2. Synchronization of a single group. (a) Time evolution of the amplitude $\langle S^+\rangle$ below and above the critical coupling strength V_c. (b) Time-averaged long-time limit amplitude $|\langle S^+\rangle|_t$ and coherences, showing a sharp transition at V_c. Parameters in (a) and (b): $\gamma_+ = \gamma_-/2$ and $K = 0$. (c) Order parameter $|\langle S^+\rangle|_t$ as a function of the coupling strength V and γ_+/γ_- as a gray-scale image for asymmetry parameter $K = 0$. The black dashed line displays the corresponding critical coupling strength obtained from a stability analysis. The orange and blue lines show the critical coupling strengths for $K/(\gamma_- + \gamma_+) = -1/10$ and $+1/10$, respectively. In the region γ_+/γ_- around 1, synchronization is suppressed for $K \geq 0$ due to the interference blockade; for negative values of K, the blockade vanishes and synchronization reappears, as indicated by the finite critical coupling strength for $K/(\gamma_- + \gamma_+) = -1/10$ (orange line). (d) Phase distributions $s(\phi)$ (the mean $1/2\pi$ is subtracted) for the same values of $K/(\gamma_- + \gamma_+)$ as in (c).

gain and loss rates are equal due to destructive interference [15,59,61]. Our result reveals that the wavelike character of the oscillators allowing for interference also shapes the dynamics in the macroscopic ensemble.

For a single asymmetric three-level oscillator, the interference blockade is lifted for *any* nonzero value of the asymmetry parameter K [61]. In contrast, we find that the blockade in the macroscopic ensemble is lifted *only* for $K < 0$, but persists for $K \geq 0$; see Fig. 2(c). To understand this apparent discrepancy, we examine the microscopic quantum synchronization behavior. Figure 2(d) shows the phase distribution $s(\phi)$ of a single oscillator coupled to an external drive in the steady state for various values of K. The distribution $s(\phi)$ indicates the phase response of the driven oscillator [71]. In the case $\gamma_+ = \gamma_-$ and $K = 0$, the phase shifts $\phi = 0$ and $\phi = \pi$ between oscillator and drive are equally likely. For the ensemble of oscillators, this implies that any mean field present causes each oscillator to align itself both in and out of phase with the mean field. Hence, the response of each oscillator will not amplify the coherence of the group, which leads to the absence of synchronization, i.e., the macroscopic interference blockade. For $K < 0$, however, each oscillator preferably aligns its phase with the mean field leading to synchronization of the group. On the other hand, for $K > 0$, each oscillator favors a phase shift of π with respect to the mean field, resulting in *phase frustration* that hinders synchronization. Therefore, unlike the interference blockade of a single oscillator, the macroscopic interference blockade is only lifted for negative K. For $\gamma_+ \neq \gamma_-$, we similarly find that the phase distribution tends to peak closer to $\phi = 0$ (π) for negative (positive) values of K, which is reflected by the respective critical coupling strengths shown in Fig. 2(c) being smaller (larger).

In summary, the ensemble of quantum oscillators may synchronize above a critical coupling strength, as expected from generic models of noisy classical oscillators. Importantly though, the quantum nature of the oscillators remains influential on the macroscopic scale: destructive interference manifests itself as a blockade of global synchronization. Moreover, phase frustration causes an emergent additional blockade only present in the large network.

Synchronization of two groups.—We now consider the full model where one half of the oscillators is detuned by δ from the other half. We identify three different states in the long-time limit. The first is the absence of any synchronization, indicated by both amplitudes $\langle S^+\rangle_\sigma$ vanishing. Secondly, all oscillators of both groups can fully synchronize. Thirdly, there is a state of partial synchronization where all oscillators within each group synchronize internally but not with the oscillators of the other group.

To distinguish full and partial synchronization, we compare the oscillation frequencies of both groups. For this purpose, we compute the discrete Fourier transform of the amplitudes in the long-time limit to obtain the spectra $P_\sigma(\omega) = |\mathrm{FT}\{\langle S^+\rangle_\sigma(t)\}|$ for each group. Figures 3(a) and 3(b) display the spectra as a function of the detuning δ. We set $V > V_c$ such that the oscillators are synchronized within each group. For sufficiently small detuning compared to the intergroup coupling strength, we find a fully synchronized state as indicated by the identical spectra in this regime. Since each spectrum is dominated by one frequency, we continue the analysis using the two frequencies at which the spectra peak, $\omega_\sigma = \mathrm{argmax}_\omega P_\sigma(\omega)$. The frequency difference $\omega_A - \omega_B$ between the two groups is displayed in Fig. 3(c). At small δ, the frequencies are equal and the two groups are synchronized, while for large detunings, ω_A and ω_B differ by δ. This corresponds to the dynamics described by the Adler equation [5,77] for classical phase oscillators. To further demonstrate this correspondence, we show the frequency difference in Fig. 3(d) as a function of the intergroup coupling strength. For $V_{AB} < V$, both individually synchronized groups of oscillators can be regarded as two large oscillators that

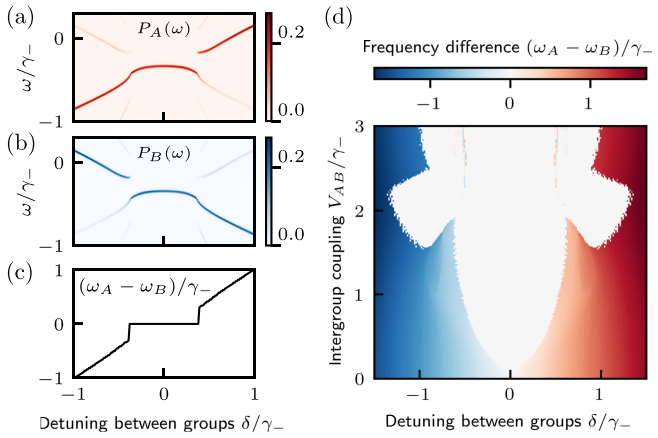

FIG. 3. Synchronization of two groups. (a),(b) Spectra $P_\sigma(\omega)$ for $\sigma = A, B$ obtained via Fourier transform of the time evolution of $\langle S^+ \rangle_\sigma$ as a function of detuning δ. (c) Difference of the two dominant frequencies, $\omega_A - \omega_B$. (d) Frequency difference between the two groups as a function of detuning δ and intergroup coupling V_{AB}. Parameters: $K = 0$, $V = 2\gamma_+ = \gamma_-$ (such that $V > V_c$). (a)–(c): $V_{AB} = V/2$.

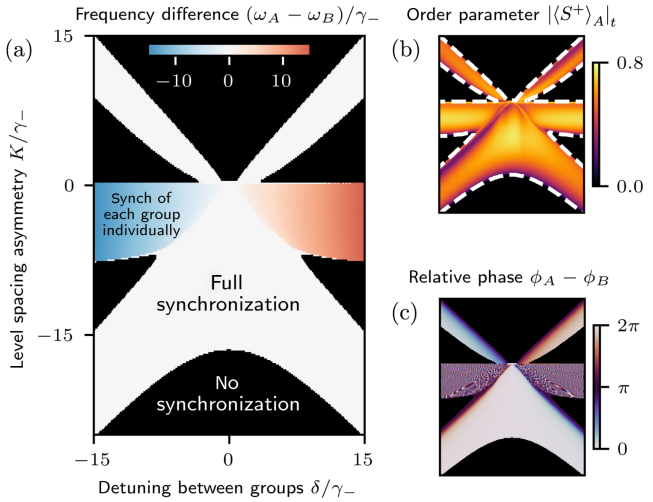

FIG. 4. Macroscopic quantum synchronization blockade. Panels (a)–(c) show the frequency difference, the order parameter, and the relative phase, respectively, as a function of detuning δ and asymmetry parameter K. The phase ϕ_σ for $\sigma = A, B$ is the argument of $\langle S^+ \rangle_\sigma$ in the long-time limit. In (b) and (c), δ and K have the same range as in (a). In (a) and (c), black color indicates regions where the order parameter vanishes, i.e., synchronization is absent. When each group synchronizes individually, i.e., in the blue and red regions in (a), the relative phase in (c) takes arbitrary values since there is no fixed phase relation between the two groups. Parameters: $V_{AB} = V = 2\gamma_+ = \gamma_-$.

synchronize when their coupling is larger than their detuning. In this regime, the microscopic details are irrelevant and the behavior matches that of generic synchronization models. Specifically, we observe an Arnold tongue [5], i.e., the locking range grows with increasing coupling strength. For $V_{AB} > V$, the intergroup coupling dominates, so that the analogy of two large coupled oscillators fails and the spectra show more than one relevant frequency component [71].

The previous analysis was done for a symmetric three-level structure, i.e., $K = 0$. We now vary the asymmetry parameter K in addition to the detuning δ and present the resulting phase diagram in Fig. 4. Remarkably, for large $|K|/\gamma_-$, we find synchronization only if $|\delta| \sim |K|$, while synchronization is absent for δ around zero. This is a macroscopic manifestation of the quantum synchronization blockade [32]: the two groups synchronize when they are distinct, but not if they are similar. This is in contrast to the expected behavior that a greater similarity of oscillators increases their tendency to synchronize [see Fig. 3(d)]. The absence of synchronization is caused by the discrete energy spectrum of the oscillators. The effect of the coupling between two oscillators is suppressed when $|K|$ significantly differs from $|\delta|$ because the dominant transitions are off-resonant [71]. Only *close to* the resonances $K = \delta$ and $K = -\delta$, there is strong phase alignment of the two oscillators. This explains the microscopic synchronization blockade; however, it does not yet fully capture the macroscopic quantum synchronization blockade, since we find synchronization only *below* the lines $K = \delta$ and $K = -\delta$. Below these lines, oscillators of different groups tend to align their phases, while above, they favor opposite phases [71]. This becomes apparent in the phase difference of the two groups; see Fig. 4(c), which shows the relative phase approaching π close to the diagonals. Each oscillator reacts to the mean fields of both groups, such that their influence cancels if they have opposite phases. This constitutes another instance of phase frustration, which in this case results in an additional blockade of synchronization for $K > \delta$.

To summarize the analysis of two groups, parts of their dynamics can be understood as a typical synchronization transition. In general, however, the quantum properties change the dynamics significantly: we demonstrated a blockade of global synchronization resulting from the quantized nature of the oscillators. Moreover, an extended blockade of synchronization emerges in the ensemble not present in the case of two coupled oscillators.

Experimental considerations.—Possible experimental realizations include superconducting circuits [32,78] and trapped ions [13,32,38]. We discuss these two implementations and general requirements to observe the phenomena presented in our work in [71]. We also address finite-size effects, and show that the lifetime of the coherence in a single group increases linearly with the number of oscillators [71]. Since global synchronization can persist for finite-range interactions in networks of classical oscillators [4] and quantum oscillators [22], we expect the all-to-all coupling that we assumed not to be essential.

Conclusion.—While quantum effects in synchronization have been studied at the level of few coupled oscillators, it

has remained an open question whether these effects remain when increasing the number of oscillators. To address this issue, we investigated the synchronization behavior of two macroscopically large groups of reactively coupled quantum limit-cycle oscillators. We demonstrated that quantum effects in synchronization persist on a macroscopic scale: for a single group, destructive interference manifests itself as a blockade of collective synchronization if gain and loss rates are comparable; for two detuned groups of oscillators with an asymmetric level structure, their quantized nature counterintuitively leads to synchronization of dissimilar groups. We also identified certain aspects of the dynamics that can be understood from classical generic synchronization models: for a single group, the transition to synchronization necessitates a critical coupling strength to overcome disorder through quantum fluctuations; for two groups of oscillators with a symmetric level structure in the regime of small intergroup coupling strength, their dynamics can be understood as the synchronization of two classical phase oscillators. Finally, we uncovered emergent behavior only present in the macroscopic ensemble: phase frustration, i.e., oscillators antialigning their phases, suppresses the global coherence and results in the absence of collective synchronization.

We expect our work to stimulate the exploration of other intriguing aspects in many-body quantum synchronization beyond classical expectations. Additionally, our results further connect synchronization to dissipative quantum phase transitions, such as superradiance and time crystals.

We would like to thank M. Koppenhöfer and N. Lörch for stimulating discussions. Furthermore, we acknowledge the use of QuTiP [79] and QuantumCumulants.jl [80], as well as financial support from the Swiss National Science Foundation individual grant (Grant No. 200020 200481).

[1] G. H. Goldsztein, A. N. Nadeau, and S. H. Strogatz, Chaos **31**, 023109 (2021).
[2] J. B. Buck, Q. Rev. Biol. **13**, 301 (1938).
[3] S. H. Strogatz, D. Abrams, F. McRobie, B. Eckhardt, and E. Ott, Nature (London) **438**, 43 (2005).
[4] J. A. Acebrón, L. L. Bonilla, C. J. Pérez Vicente, F. Ritort, and R. Spigler, Rev. Mod. Phys. **77**, 137 (2005).
[5] A. Pikovsky, M. Rosenblum, and J. Kurths, *Synchronization: A Universal Concept in Nonlinear Sciences*, Cambridge Nonlinear Science Series (Cambridge University Press, Cambridge, England, 2001).
[6] S. H. Strogatz, *Sync: The Emerging Science of Spontaneous Order* (Hyperion, New York, 2003).
[7] K. Okuda and Y. Kuramoto, Prog. Theor. Phys. **86**, 1159 (1991).
[8] E. Montbrió, J. Kurths, and B. Blasius, Phys. Rev. E **70**, 056125 (2004).
[9] O. V. Zhirov and D. L. Shepelyansky, Eur. Phys. J. D **38**, 375 (2006).
[10] A. Chia, L. C. Kwek, and C. Noh, Phys. Rev. E **102**, 042213 (2020).
[11] L. Ben Arosh, M. C. Cross, and R. Lifshitz, Phys. Rev. Res. **3**, 013130 (2021).
[12] M. Ludwig and F. Marquardt, Phys. Rev. Lett. **111**, 073603 (2013).
[13] T. E. Lee and H. R. Sadeghpour, Phys. Rev. Lett. **111**, 234101 (2013).
[14] S. Walter, A. Nunnenkamp, and C. Bruder, Phys. Rev. Lett. **112**, 094102 (2014).
[15] A. Roulet and C. Bruder, Phys. Rev. Lett. **121**, 053601 (2018).
[16] Á. Parra-López and J. Bergli, Phys. Rev. A **101**, 062104 (2020).
[17] A. W. Laskar, P. Adhikary, S. Mondal, P. Katiyar, S. Vinjanampathy, and S. Ghosh, Phys. Rev. Lett. **125**, 013601 (2020).
[18] V. R. Krithika, P. Solanki, S. Vinjanampathy, and T. S. Mahesh, Phys. Rev. A **105**, 062206 (2022).
[19] L. Zhang, Z. Wang, Y. Wang, J. Zhang, Z. Wu, J. Jie, and Y. Lu, Phys. Rev. Res. **5**, 033209 (2023).
[20] M. Koppenhöfer, C. Bruder, and A. Roulet, Phys. Rev. Res. **2**, 023026 (2020).
[21] M. Xu, D. A. Tieri, E. C. Fine, J. K. Thompson, and M. J. Holland, Phys. Rev. Lett. **113**, 154101 (2014).
[22] B. Zhu, J. Schachenmayer, M. Xu, F. Herrera, J. G. Restrepo, M. J. Holland, and A. M. Rey, New J. Phys. **17**, 083063 (2015).
[23] A. Mari, A. Farace, N. Didier, V. Giovannetti, and R. Fazio, Phys. Rev. Lett. **111**, 103605 (2013).
[24] B. Bandyopadhyay and T. Banerjee, Phys. Rev. E **107**, 024204 (2023).
[25] D. Witthaut, S. Wimberger, R. Burioni, and M. Timme, Nat. Commun. **8**, 14829 (2017).
[26] S. Lorenzo, B. Militello, A. Napoli, R. Zambrini, and G. M. Palma, New J. Phys. **24**, 023030 (2022).
[27] C. Davis-Tilley, C. K. Teoh, and A. D. Armour, New J. Phys. **20**, 113002 (2018).
[28] C. W. Wächtler and G. Platero, Phys. Rev. Res. **5**, 023021 (2023).
[29] W. Li, C. Li, and H. Song, Phys. Rev. E **95**, 022204 (2017).
[30] K. Ishibashi and R. Kanamoto, Phys. Rev. E **96**, 052210 (2017).
[31] N. Lörch, E. Amitai, A. Nunnenkamp, and C. Bruder, Phys. Rev. Lett. **117**, 073601 (2016).
[32] N. Lörch, S. E. Nigg, A. Nunnenkamp, R. P. Tiwari, and C. Bruder, Phys. Rev. Lett. **118**, 243602 (2017).
[33] S. Dutta and N. R. Cooper, Phys. Rev. Lett. **123**, 250401 (2019).
[34] H. Eneriz, D. Z. Rossatto, F. A. Cardenas-Lopez, E. Solano, and M. Sanz, Sci. Rep. **9**, 19933 (2019).
[35] Y. Shen, W.-K. Mok, C. Noh, A. Q. Liu, L.-C. Kwek, W. Fan, and A. Chia, Phys. Rev. A **107**, 053713 (2023).
[36] G. L. Giorgi, F. Galve, G. Manzano, P. Colet, and R. Zambrini, Phys. Rev. A **85**, 052101 (2012).
[37] V. Ameri, M. Eghbali-Arani, A. Mari, A. Farace, F. Kheirandish, V. Giovannetti, and R. Fazio, Phys. Rev. A **91**, 012301 (2015).
[38] M. R. Hush, W. Li, S. Genway, I. Lesanovsky, and A. D. Armour, Phys. Rev. A **91**, 061401(R) (2015).

[39] V. M. Bastidas, I. Omelchenko, A. Zakharova, E. Schöll, and T. Brandes, Phys. Rev. E **92**, 062924 (2015).
[40] C. Davis-Tilley and A. D. Armour, Phys. Rev. A **94**, 063819 (2016).
[41] T. Weiss, A. Kronwald, and F. Marquardt, New J. Phys. **18**, 013043 (2016).
[42] W. Li, W. Zhang, C. Li, and H. Song, Phys. Rev. E **96**, 012211 (2017).
[43] T. Weiss, S. Walter, and F. Marquardt, Phys. Rev. A **95**, 041802(R) (2017).
[44] L. Du, C.-H. Fan, H.-X. Zhang, and J.-H. Wu, Sci. Rep. **7**, 15834 (2017).
[45] E. Amitai, M. Koppenhöfer, N. Lörch, and C. Bruder, Phys. Rev. E **97**, 052203 (2018).
[46] S. Sonar, M. Hajdušek, M. Mukherjee, R. Fazio, V. Vedral, S. Vinjanampathy, and L.-C. Kwek, Phys. Rev. Lett. **120**, 163601 (2018).
[47] F. A. Cardenas-Lopez, M. Sanz, J. C. Retamal, and E. Solano, Adv. Quantum Technol. **2**, 1800076 (2019).
[48] N. Jaseem, M. Hajdušek, P. Solanki, L.-C. Kwek, R. Fazio, and S. Vinjanampathy, Phys. Rev. Res. **2**, 043287 (2020).
[49] N. Es'haqi-Sani, G. Manzano, R. Zambrini, and R. Fazio, Phys. Rev. Res. **2**, 023101 (2020).
[50] A. Cabot, G. L. Giorgi, and R. Zambrini, New J. Phys. **23**, 103017 (2021).
[51] F. Schmolke and E. Lutz, Phys. Rev. Lett. **129**, 250601 (2022).
[52] P. Solanki, N. Jaseem, M. Hajdušek, and S. Vinjanampathy, Phys. Rev. A **105**, L020401 (2022).
[53] B. Bandyopadhyay and T. Banerjee, Phys. Rev. E **106**, 024216 (2022).
[54] B. Buca, C. Booker, and D. Jaksch, SciPost Phys. **12**, 097 (2022).
[55] Y. Kato and H. Nakao, New J. Phys. **25**, 023012 (2023).
[56] C.-G. Liao, R.-X. Chen, H. Xie, M.-Y. He, and X.-M. Lin, Phys. Rev. A **99**, 033818 (2019).
[57] H. W. H. Lau, J. Davidsen, and C. Simon, Sci. Rep. **13**, 8590 (2023).
[58] A. Roulet and C. Bruder, Phys. Rev. Lett. **121**, 063601 (2018).
[59] M. Koppenhöfer and A. Roulet, Phys. Rev. A **99**, 043804 (2019).
[60] N. Jaseem, M. Hajdušek, V. Vedral, R. Fazio, L.-C. Kwek, and S. Vinjanampathy, Phys. Rev. E **101**, 020201(R) (2020).
[61] P. Solanki, F. M. Mehdi, M. Hajdušek, and S. Vinjanampathy, Phys. Rev. A **108**, 022216 (2023).
[62] A. Delmonte, A. Romito, G. E. Santoro, and R. Fazio, Phys. Rev. A **108**, 032219 (2023).
[63] T. Murtadho, S. Vinjanampathy, and J. Thingna, Phys. Rev. Lett. **131**, 030401 (2023).
[64] R. J. Valencia-Tortora, S. P. Kelly, T. Donner, G. Morigi, R. Fazio, and J. Marino, Phys. Rev. Res. **5**, 023112 (2023).
[65] H. Spohn, Rev. Mod. Phys. **52**, 569 (1980).
[66] T. E. Lee, C.-K. Chan, and S. Wang, Phys. Rev. E **89**, 022913 (2014).
[67] Y. Kuramoto, in *International Symposium on Mathematical Problems in Theoretical Physics*, edited by H. Araki (Springer Berlin Heidelberg, Berlin, Heidelberg, 1975), p. 420.
[68] F. Iemini, A. Russomanno, J. Keeling, M. Schirò, M. Dalmonte, and R. Fazio, Phys. Rev. Lett. **121**, 035301 (2018).
[69] K. Tucker, B. Zhu, R. J. Lewis-Swan, J. Marino, F. Jimenez, J. G. Restrepo, and A. M. Rey, New J. Phys. **20**, 123003 (2018).
[70] P. Kirton, M. M. Roses, J. Keeling, and E. G. Dalla Torre, Adv. Quantum Technol. **2**, 1800043 (2019).
[71] See Supplemental Material at http://link.aps.org/supplemental/10.1103/PhysRevLett.131.190402, which includes Refs. [72–76], for details on the microscopic results, additional figures, a discussion of finite-size effects and experimental requirements, as well as more information on the methods.
[72] R. Kubo, J. Phys. Soc. Jpn. **17**, 1100 (1962).
[73] A. Oppenheim, R. Schafer, and J. Buck, *Discrete-Time Signal Processing*, Prentice Hall International Editions (Prentice Hall, New York, 1999).
[74] J. Majer, J. M. Chow, J. M. Gambetta, J. Koch, B. R. Johnson, J. A. Schreier, L. Frunzio, D. I. Schuster, A. A. Houck, A. Wallraff, A. Blais, M. H. Devoret, S. M. Girvin, and R. J. Schoelkopf, Nature (London) **449**, 443 (2007).
[75] T. Onodera, E. Ng, and P. L. McMahon, npj Quantum Inf. **6**, 48 (2020).
[76] D. Leibfried, R. Blatt, C. Monroe, and D. Wineland, Rev. Mod. Phys. **75**, 281 (2003).
[77] R. Adler, Proc. IRE **34**, 351 (1946).
[78] S. E. Nigg, Phys. Rev. A **97**, 013811 (2018).
[79] J. Johansson, P. Nation, and F. Nori, Comput. Phys. Commun. **184**, 1234 (2013).
[80] D. Plankensteiner, C. Hotter, and H. Ritsch, Quantum **6**, 617 (2022).